FAILURE TESTING AND TEST SIMULATION OF THE ARIANE 5 EPC BME ACTUATOR BRACKETS

J. Hoogendoorn, J.F. Koorevaar
H.Hoogendoorn@dutchspace.nl, J.Koorevaar@dutchspace.nl
Dutch Space B.V. an EADS Astrium Company
P.O. Box 32070
2303 DB Leiden
The Netherlands

OVERVIEW

The payload of ARIANE 5 is still increasing. More thrust is generated by the Vulcain II engine that powers the first stage (EPC). The steering of this engine is done by two actuators each mounted on a double lug bracket on the Bâti Moteur Equipé (BME), developed by Dutch Space in the Netherlands. The ultimate load that these attachments can handle has been determined by a test programme involving two tension and two compression tests. Both these tests have also been simulated using the non-linear Finite Element Method (FEM) software ABAQUS version 6.5-4.

The simulation has been used for predictions of structural failure. The loads in the Finite Element model (FE model were corrected for the deviations in dimensions (tolerance ranges) and material specification to be able to predict the test results.

The model was designed to predict a correct failure load and mode. The choice of material model was important. The specifications for the material were a given minimum yield and ultimate stress and ultimate strain value. With these values the “deformation plasticity” material model was chosen. This material model is also known as the Ramberg-Osgood model. For practical reasons all connection bolts have been modelled as rigid elements.

During the correlation process it was found that the lug strain FE values were close to the test values, but that the global stiffness deviated. This paper will describe the test programme, the design of the FE model and the correlation of the FE and test results.

1. INTRODUCTION

Since the start of the development of a European family of launch vehicles, Dutch Space has had turnkey responsibility for the design, analysis, development, qualification and manufacture of the third stage engine frame for Ariane 1 through 4. Until end of utilization of the Ariane 4 launcher in 2002, Dutch Space has delivered over 140 sets of engine frames meeting the cost and schedule requirements of the customer. The highest production rate achieved was twelve sets per year.

In addition to Ariane 1 through 4, Dutch Space was selected for the Ariane 5 Main Engine Frame, one of the most complex structural systems of the Ariane 5 launcher. Up to 2003 Dutch Space had delivered over thirty sets of flight models. In 2004 the contract was signed for delivery of another thirty sets to be delivered in the period up to 2009. Currently, negotiations are underway for a further batch of as many as 35 Ariane 5’s.

FIG 1. Overview of the Ariane 5 EPC BME.

The Ariane 5 EPC BME can be subdivided in four parts, where the lower part is called the cross. The cross is shown in figure 2 and can also be seen in figure 1. The Vulcain II engine is mounted to the cross. The steering actuators are also connected to the cross via the actuator brackets which can be seen in figure 2.

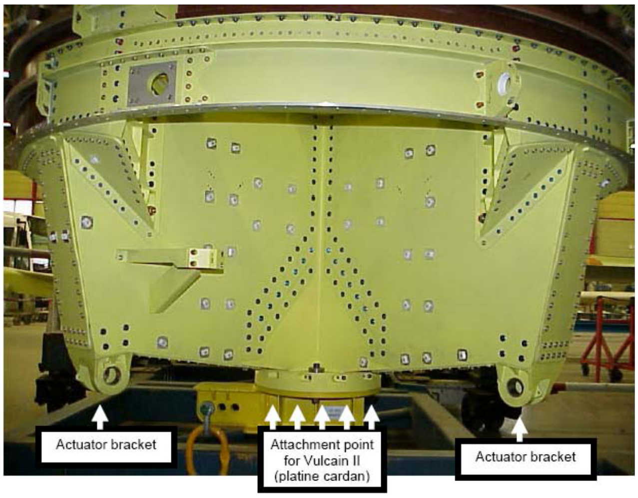

FIG 2. Actuator brackets on the cross of the Ariane 5 EPC BME.

The Ariane 5 first stage is powered by the Vulcain II engine. The Vulcain II loads were increased, which also resulted in higher actuator loads. It was necessary to know more accurately what the maximum carrying capacity of the actuator bracket was. The test programme was done in the frame of A5 ECA development by ESA, CNES, Astrium-ST and Dutch Space.

2. TEST PROGRAMME

The test programme consisted of four failure tests on four identical test articles and corresponding FE analyses. The test article was a sub part of the engine frame with special modifications for practical reasons. The four failure tests were two tension load cases and two compression load cases. All the load cases were applied at the same load angle. The FE analyses performed are non-linear static analyses using ABAQUS/Standard software version 6.5-4. Preliminary analysis results were used for determining strain gauge locations and used as input for the test procedure.

During each test three load sequences were applied:

1) Load case up to limit load level.
2) Load case up to yield load level.
3) Load case up to failure of the test article or up to the maximum load cell load.

Failure can be defined as rupture of a lug and/or failure of fasteners. In the compression load case, buckling was also seen as failure because it results in a sudden loss of stiffness. The second load case should not give residual strains. A limit of five percent of the maximum occurred strain at that location was used for this criterion in this test programme. The failure of the test article should occur in the actuator bracket or its connections to the structure but not in the connections of the test article to the test set-up, nor in the test set-up itself.

Measurements during the tests were done with lasers and strain gauges. In total fifteen displacements and thirty nine strains were measured. The strain gauges, single strain gauges and rosettes, were also used during testing for monitoring the behaviour of the test articles. Test results of nine displacements and fourteen strains were compared with the analysis results of the FE model.

All test results and FE analyses are documented and are used in the further development of the Ariane 5 EPC BME.

3. FE MODEL

The FE model was generated in ABAQUS/CAE by importing CATIA V5 geometry. Figure 3 shows an overview of the mesh of the whole FE model. Figure 4 shows the geometry of the actuator bracket and the parts used for connection to the actuator. The actuator bracket itself (nr. 1, Figure 4) and parts of the plates connected to the actuator bracket (nr. 6, 7 and 10 in figure 5) were modelled by solid elements, all other plates by shell elements and the pin through the bracket (nr. 4 in figure 4) by beam elements.

It was first attempted to get a solid mesh of hexagonal elements for the actuator bracket. But due to the complex structure of the bracket it was not possible and a 10-noded tetrahedral element mesh was generated with success. The bushes (nr. 2 and 3 in figure 4) were modelled by rigid bodies.

Contact was only modelled between the bushes and the lugs of the actuator bracket as it was anticipated that the failure would start in this area. The other contact areas in the test set-up were tied, connected or coupled to reduce the CPU time. The contact areas consisted of the discrete rigid bushes and deformable aluminium lugs. The normal behaviour in the contact algorithm was assumed to be hard with a default stiffness. The contact modelling also modelled friction. The friction coefficient between steel and aluminium was chosen to be 0.5. One bush (nr. 3 in figure 4) was also connected to the actuator lug to prevent movement sideways along the pin.

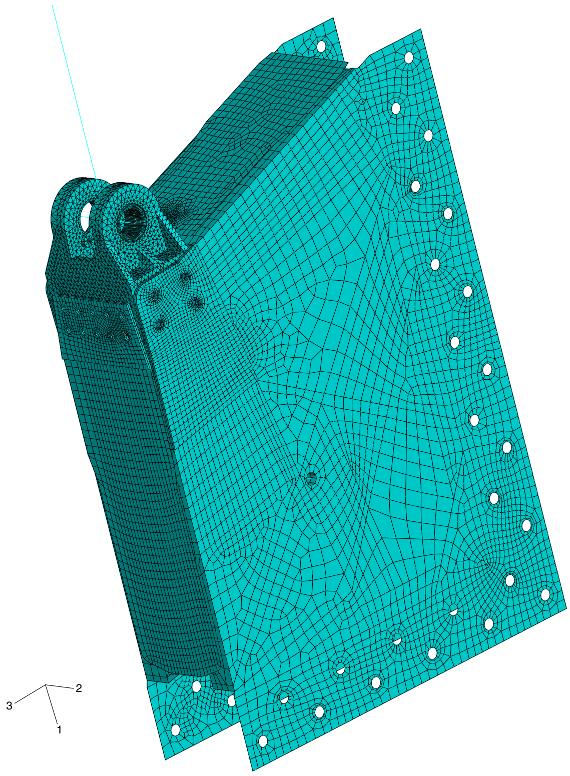

FIG 3. Mesh of the FE model.

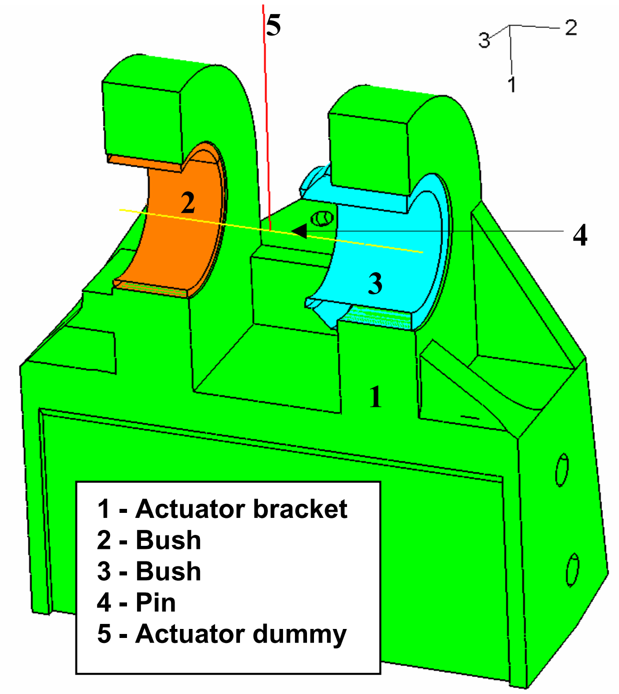

FIG 4. Cross section of the actuator bracket and its components.

The pin was in reality thick in comparison to its length but despite the high thickness-to-length ratio the pin was modelled by linear beam elements known as a linear Timoshenko shear flexible beam which takes shear deformation into account. A full solid model of the pin would be more accurate but this would have significantly increased calculation time.

The interaction between the bushes and the pin was modelled by connectors. Connectors are special elements which connect 2 points. The modelled connectors between the pin and the bushes always have one point located in the middle of the bush (cylindrical and its rotation axis) and the other point at the same location on the pin. The interaction between one bush (nr. 2 in figure 4) and the pin was modelled by a combined “slot” and “align” connector. The pin could move through the bush and did not introduce a non-existing boundary condition. The other bush (nr. 3 in figure 4) was connected by a combined “join” and “revolute” connector. The pin was connected to the bush and could not slide but was able to revolve on its axis.

The interaction between the actuator bracket and the “backup” structure (nr. 6 to 10 in figure 5) were modelled by connectors. Each fastener was modelled by one rigid connector. The rigid connector was connected to the corresponding plate by a constraint which was a kinematical coupling constrained in all six directions. This meant that the nodes on the surface of the hole followed the translations (and rotations) of the reference node at the rigid connector.

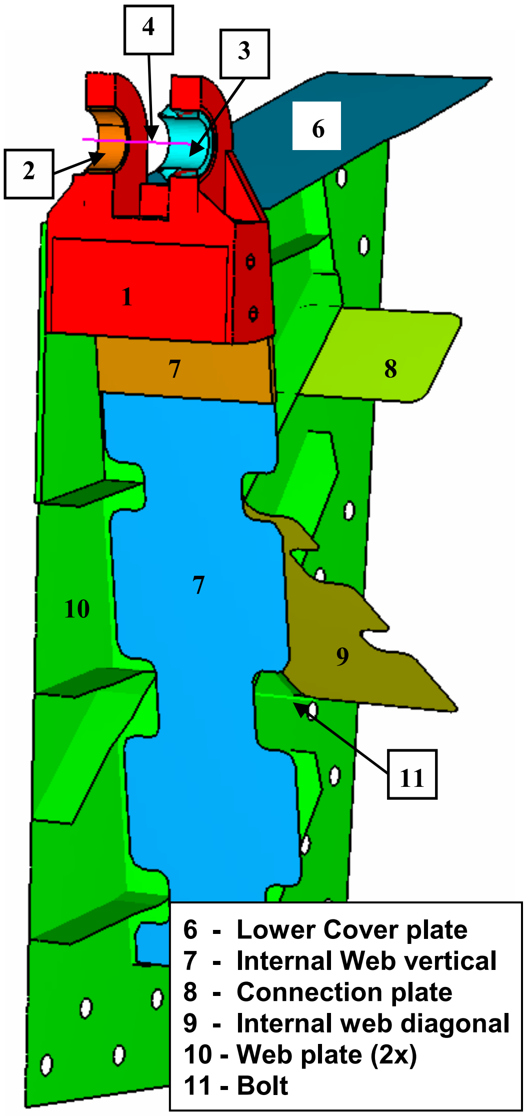

FIG 5. Plates in the test article connected to the actuator bracket.

4. MATERIAL MODELS

Two different material models were used: a linear elastic model and a nonlinear model. The nonlinear material model was an important choice as plasticity had to be modelled correctly to be able to model failure accurately. ABAQUS software provides a material model called Deformation Plasticity. The Deformation Plasticity material model is also known as Ramberg-Osgood. The material behaviour described by this model is nonlinear at all stress levels, but the nonlinearity becomes significant only at stress magnitudes approaching or exceeding the yield stress, see figure 5. The Young’s modulus, Poisson ratio, yield stress and hardening parameter were known. The yield offset was calculated by fitting the yield offset α in the equation:

$$E \cdot \varepsilon = \sigma + \alpha \left(\frac{|\sigma|}{\sigma^0} \right)^{n-1} \sigma$$

With the maximum stress and strain situation α was the only unknown parameter and could be determined.

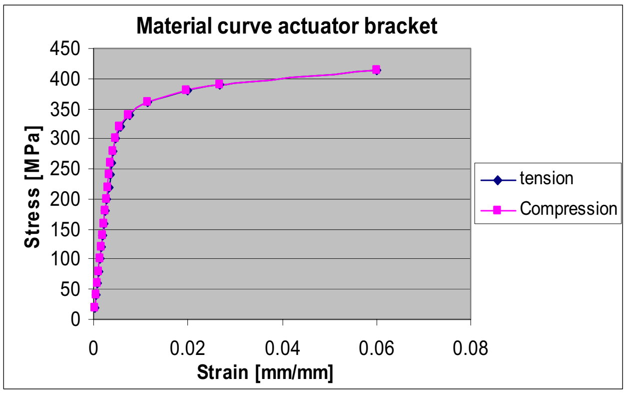

FIG 6. Material stress vs. strain curve for deformation plasticity model with fitted alpha value.

5. TEST RESULTS

When looking at all four tests as a whole there were two important events that took place. The first is failure of one lug during the first tension test (figure 7 and 8) and the second was that HiLok damage at the connection of the actuator bracket with the shear webs occurred during all four tests (figure 9).

It was expected that both test articles subjected to tension would fail. But only the test article of the first tension test failed as expected. All other test articles did not fail but carried the maximum possible test load. For the compression load case it was expected that the lug would not fail but buckling or HiLok failure was expected. Neither of the two test articles subjected to compression failed, but HiLok damage did occur.

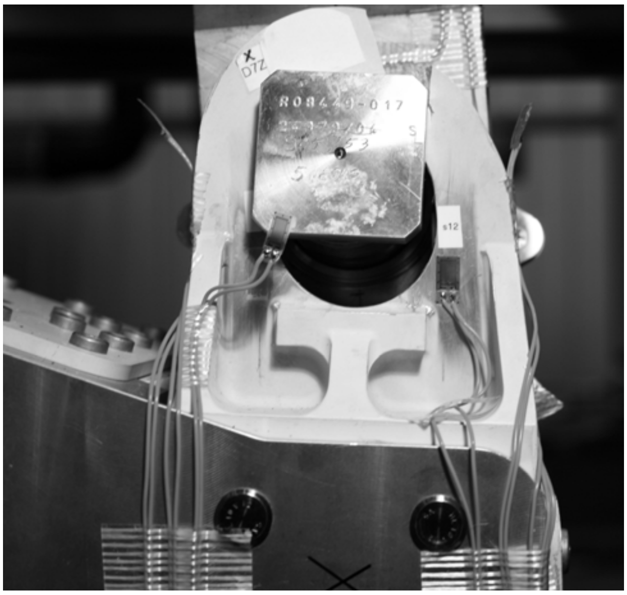

FIG 7. The actuator bracket with failed lug (side view).

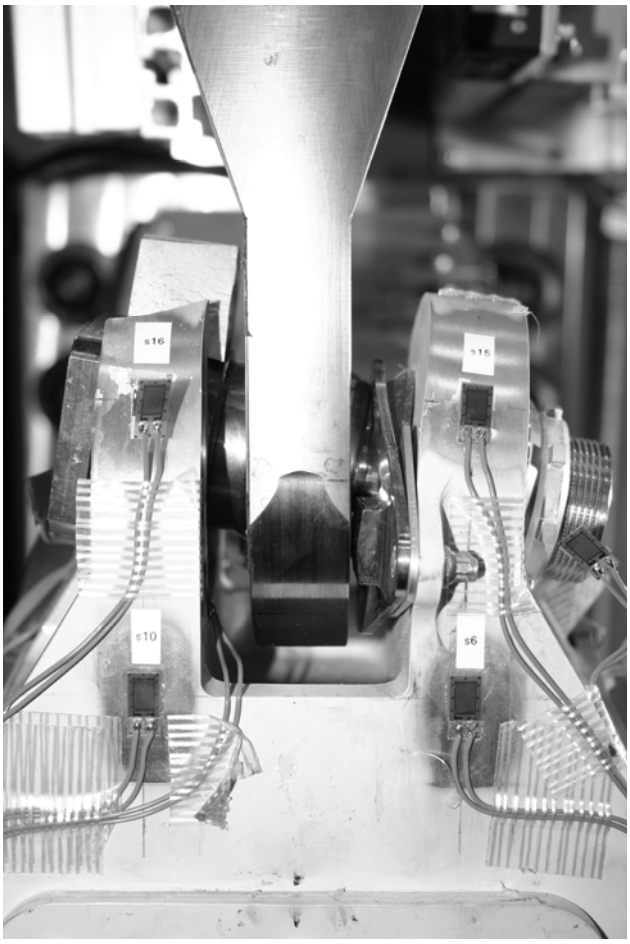

FIG 8. The actuator bracket with left lug failed (front view).

After closer inspection of the test article following completion of the first tension test, it was discovered that not only had the actuator bracket lug failed, but three of the HiLoks connecting the actuator bracket to the web plates (nr 10 in figure 5) had been damaged at a lower load level than the lug failure (see figure 9). Since the focus was on the actuator lug this damage had not been noticed during the test itself.

However, based on the results of the second tension test parallels could be drawn between the two tension tests. During the second tension test two additional strain gauges were located between the HiLoks that were damaged. By comparing the graphs of strain gauges it was possible to deduce the levels at which the HiLoks were damaged. These results in the graphs were confirmed by the available video of the second tension test.

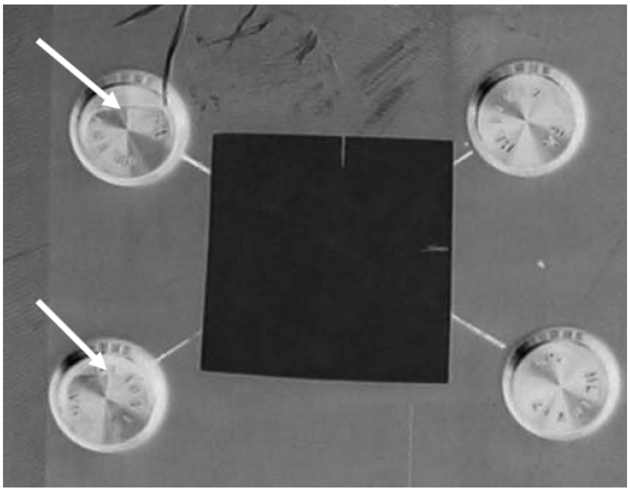

FIG 9. HiLok damage (negative view, arrows point to damage).

6. CORRELATION OF FE AND TEST RESULTS

After the first test the failure load predictions and failure mode of the FE model were very similar and it was agreed that no intermediate correlation was needed. Initially this had been planned if the prediction and test results did not correspond. Only after all four tests had been finished was a correlation between the test programme and FE model done.

It was shown that the lugs of the actuator bracket are the weakest point in the tested structure (as predicted). The correlation in this location was consequently considered the most important. Two strain gauges (S.13.S.Y and S.14.S.Y in figure 10) on the lugs were compared. The comparison also considered the nonlinear behaviour of the lugs. In figure 8 it can be seen that the strain gauges were located close to the area where the failure took place.

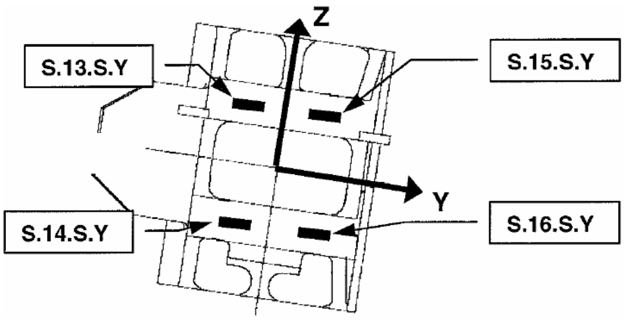

FIG 10. Strain gauge locations on the lugs of the actuator bracket.

Although the FE model was based on nominal thicknesses and nominal material properties the correlation has been based on uncorrected test data for these parameters. This has been done because the correction factors for the parameters differed also and no consistent correction factor could be found.

Figure 11 shows the FE and test results of the lug that was still intact after the test. It could be seen that the two test values differed a lot and the FE results were almost identical to the measured values of the second tension test. Figure 12 shows the FE and test results of the lug that failed during the test. It can be seen that the two test values differed a lot (compare S.14.S.Y Test A vs. S.14.S.Y Test C) but the FE results were in-between both measured test values even far in the nonlinear area.

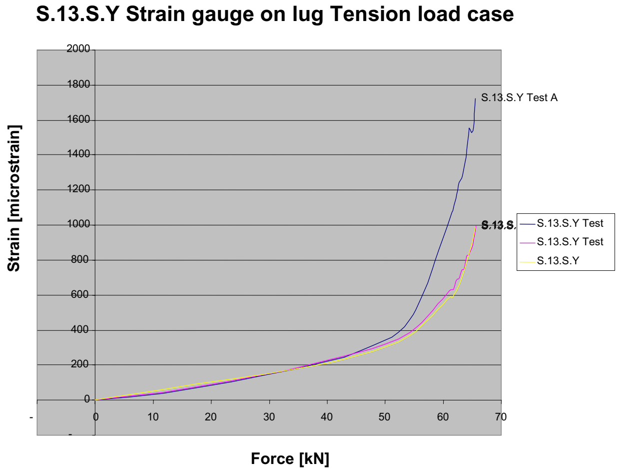

FIG 11. FE and test data compared in one diagram for strain gauge S.13.S.Y.

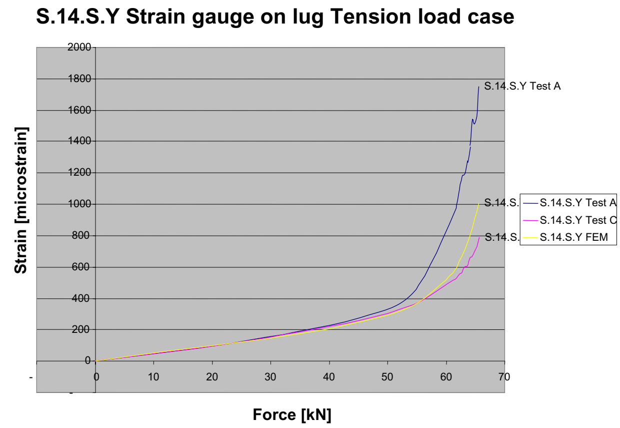

FIG 12. FE and test data compared in one diagram for strain gauge S.13.S.Y.

The strains in the plates connected to the actuator bracket were also compared. The correlation of these strains was less good. In the FE model fasteners between the actuator bracket and plates were modelled as rigid beams. But in reality, the diameter of the fasteners differed and therefore the fasteners had different stiffness. The FE strains at one plate (S.23.R.XZ in figure 13) were higher than the test results, see figure 15. But at the web plates (S.22.R.XY in figure 13) the FE strains were lower than the test values, see figure 14. From this it could be concluded that the load distribution from the actuator bracket to the plates was not completely accurate in the FE model. The strains near the test set-up connections were similar and correlated quite well.

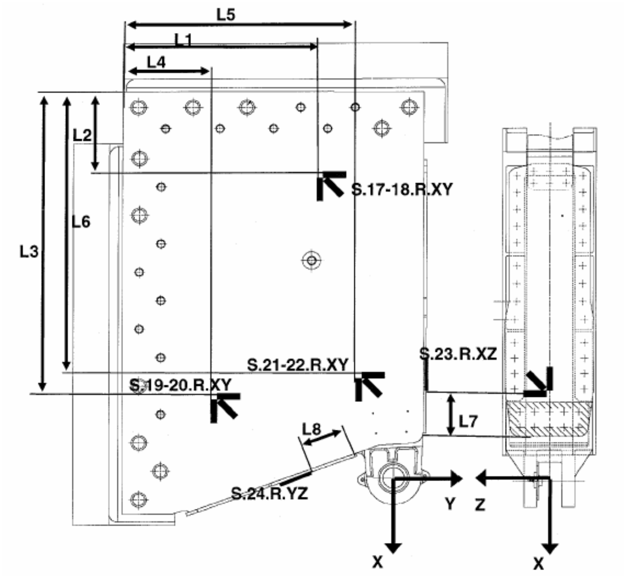

FIG 13. Strain gauge locations on the plates connected to the actuator bracket.

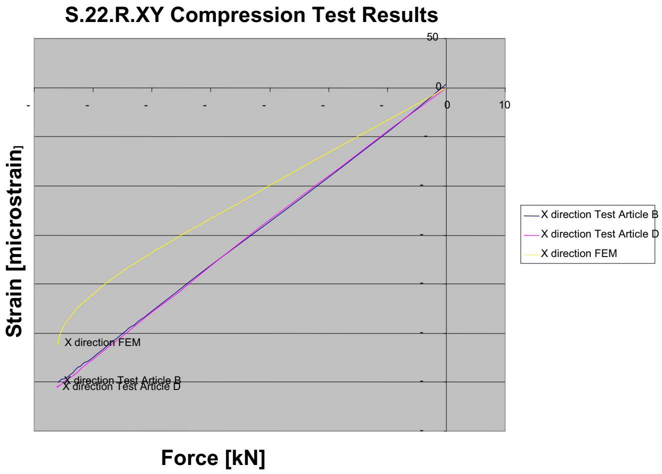

FIG 14. FE and test values of strain gauge at location S.22.R.XY.

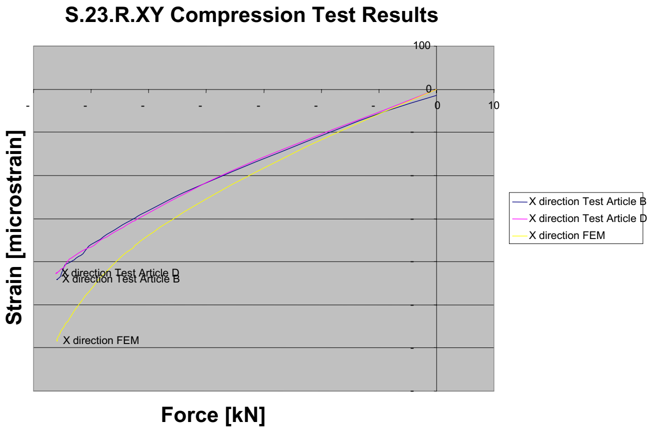

FIG 15. FE and test values of strain gauge at location S.23.R.XZ.

7. CONCLUSION

The test programme was executed successfully. The actuator bracket was stronger than initially thought.

The FE model correlates well with the test results. For the rigid fasteners a different way of modelling may be necessary, which can take the different stiffness of the connections into account.

8. ACKNOWLEDGEMENTS

The authors are grateful to CNES, Astrium-ST and Dutch Space for permission to publish this paper. Any views expressed are those of the authors and not necessarily those of Dutch Space.